Bioresource Technology 382 (2023) 129120

Contents lists available at ScienceDirect

Bioresource Technology

journal homepage: www.elsevier.com/locate/biortech

Revealing mechanism and influence of microalgae cells' periodical auto-agglomeration induced by high concentration of carbon dioxide

Hongyan Peng [a,b,1], Yun Huang [a,b,1], Ao Xia [a,b], Xianqing Zhu [a,b], Xun Zhu [a,b], Qiang Liao [a,b,*]

[a] Key Laboratory of Low-grade Energy Utilization Technologies and Systems, Chongqing University, Ministry of Education, Chongqing 400044, China
[b] Institute of Engineering Thermophysics, School of Energy and Power Engineering, Chongqing University, Chongqing 400044, China

HIGHLIGHTS

- Microalgae periodical auto-agglomeration induced by high concentration of CO_2.
- Auto-agglomeration at adaptation phase helped cells to resistance high CO_2.
- 100% auto-agglomeration at stabilization phase benefited for biomass harvesting.
- Cells' auto-agglomeration at the stabilization phase caused by lamellar EPS.
- Microalgae biomass concentration increased 18.2% when cultivated with 15% CO_2.

GRAPHICAL ABSTRACT

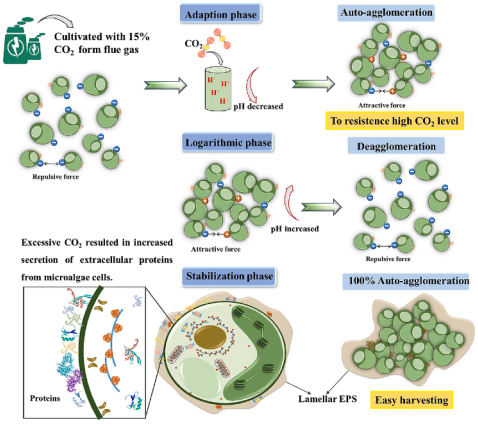

ARTICLE INFO

Keywords:
Auto-agglomeration
Carbon bio-fixation
Extracellular polymeric substances
Surface potential

ABSTRACT

The efficient cultivation of microalgae using CO_2 from flue gas can be a win-win situation for both environmental protection and energy accessibility. In general, 10–20% of CO_2 in flue gas would decrease pH and inhibit microalgae growth. However, *Chlorella sorokiniana* MB-1 under 15% CO_2 showed a periodical auto-agglomeration, which promoted microalgae growth on the contrary in this study. The maximum biomass concentration of 3.27 g L^{-1} was higher than that cultivated with an optimal CO_2 concentration. The pH decreased to 6.04 after the mixed gas with 15% CO_2 (v/v) was bubbled into medium for 0.5 h, which resulted in auto-agglomeration to protect microalgae from acidification and keep a high specific growth rate of 0.03 h^{-1}. Then the pH recovered to 7 during stabilization phase, auto-agglomeration ratio was up to 100% because of lamellar extracellular polymeric substances. Therefore, the interesting periodical agglomeration both enhanced growth and simplified harvesting.

* Corresponding author at: Institute of Engineering Thermophysics, School of Energy and Power Engineering, Chongqing University, Chongqing 400044, China.
E-mail address: lqzx@cqu.edu.cn (Q. Liao).
[1] These authors contributed equally to this work and be considered as co-first authors.

https://doi.org/10.1016/j.biortech.2023.129120
Received 9 March 2023; Received in revised form 21 April 2023; Accepted 27 April 2023
Available online 2 May 2023

1. Introduction

The increasing emissions of greenhouse gases, mainly CO_2, contribute to global warming and environmental degradation. Among the sources of CO_2 emissions, CO_2 from fossil fuel power plants account for the largest proportion amount. It was reported that 40% of global CO_2 emissions come from fossil fuel power plants, emitting nearly 32.252 Gt of CO_2 per year (IEA, 2023). In the face of the goal of carbon peaking and carbon neutralization, the development of whole-chain decarbonization technologies is the worldwide research focus, and also an indispensable development direction (Jiutian et al., 2022). Among various technologies to achieve flue gas CO_2 reduction, biological techniques attracted attention in recent years. Especially, microalgae, as a plant with higher photosynthetic efficiency (10–50 times) than terrestrial plants (Cheah et al., 2015), is driven by sunlight to convert inorganic carbon into organic carbon, while simultaneously producing renewable biomass (Ma et al., 2023; Ma et al., 2022).

Microalgae grow in the wild with CO_2 from the atmosphere (Just 0.04%). However, the concentration of CO_2 from coal-fired power plants' flue gas is usually 10–20% (Fu et al., 2022). The excessive CO_2 provided by flue gas is higher than required for microalgae growth. When CO_2 is aerated into the microalgae culture solution, the CO_2 dissolves and diffuses into the solution to synthesize carbonic acid, and the carbonic acid ionizes to produce large amounts of H^+, thus lowering the pH of the microalgae solution (Koch et al., 2013). When 20% CO_2 was used for microalgae cu6ltivation, the pH of the microalgal suspension decreased during the adaptation phase to 6 and subsequently recovered to 7.8 at the stabilization phase (Solovchenko et al., 2015). When the pH decreased, the intracellular enzyme activity of the microalgae cells was decreased, which was unfavorable for microalgae growth and carbon sequestration. (Moazami-Goudarzi & Colman, 2012).

But, changes in pH altered some of the microalgal inherent properties, including surface characteristics, physiological state, etc., changing the energy potential barriers between cells. The study of Wei et al. (2020) found that the energy potential barriers between cells disappeared when the pH of the medium decreased to 3, resulting in cells' auto-agglomeration. Microalgae cells' auto-agglomeration is closely related to medium pH (Li et al., 2021). When the medium pH increased up to 7, energy potential barriers between cells increased, and the agglomerated cells then dispersed again into the medium, this periodical auto-agglomeration happened with pH. Thus, the excessive CO_2 might result in the auto-agglomeration of microalgae cells due to the decrease of pH during the adaptation cultivation (Liu et al., 2014; Wei et al., 2020). The agglomeration of microalgae cells had the potential to enhance quorum sensing to resist stress from the environment (Mishra and Kodiveri Muthukaliannan, 2022). This cell's auto-agglomeration might be a form of self-protection from the harmful high concentration of CO_2. But how it happened is rarely known. Auto-agglomeration also makes microalgae harvesting easy. However, clumps formed by microalgae agglomerate may affect the mixing and mass, and transfer in microalgae suspension, which might inhibit microalgae growth and carbon sequestration (Yang et al., 2015). Combining these effects caused by agglomeration, it was hard to know whether auto-agglomeration during microalgal cultivation is beneficial or detrimental to microalgal growth. Therefore, to better utilize the agglomeration phenomenon to achieve high CO_2 bioconversion by microalgae, it is essential to know the mechanism and influence of microalgae cells' periodical auto-agglomeration induced by a high concentration of CO_2.

Thus, in this study, the auto-agglomeration characteristic of microalgae cultivated with 15% CO_2 at different cultivation phases, was discussed in terms of microalgae cells' surface potential, functional groups, extracellular secretions, and microalgae metabolism. Finally, the mechanism and influence of microalgae cells' periodical auto-agglomeration were discovered through the measurements. At the same time, the growth characteristics and carbon sequestration capacity of microalgae cultivated with a high concentration of CO_2 have been analyzed.

2. Materials and methods

2.1. Microalgae cultivation and measurements

The microalgae strain used in this study was *Chlorella sorokiniana* MB-1 (*C. sorokiniana* MB-1) obtained from Department of Chemical Engineering at National Cheng Kung University, Taiwan (Chen et al., 2017), and cultivated with BG-11 medium (Boussiba & Vonshak, 1991). The microalgae were cultivated in a constant temperature chamber at 25 ±1 °C. The microalgae photobioreactor was a cone-bottom column reactor made of glass with a 350 ml culture volume, and all photobioreactors operated under a light intensity of 200 $\mu mol \cdot m^{-2} \cdot s^{-1}$ provided by fluorescent lamps constantly. The mixed gas (N_2 and CO_2) was controlled by mass flowmeters (FMA-2606A, Omega, Switzerland), and mixed gas was bubbled into the microalgae suspension with a ventilation ratio of 0.1 vvm, and two CO_2 concentrations of 2% and 15% (v/v) were set.

Microalgae biomass dry weight was measured through the method described by Chang et al. (2019), and the standard curve was obtained as Eq. (1) by linearly fitting microalgae biomass dry weight with optical density.

$$X = 0.1681 \times OD_{680} - 0.0027 \quad R^2 = 0.997 \tag{1}$$

In which X (g L^{-1}) is the microalgae biomass dry weight and OD_{680} is the optical density of *C. sorokiniana* MB-1 suspension.

Microalgae specific growth rate (μ day^{-1}) and growth rate (ν mg $L^{-1}h^{-1}$) were calculated using Eqs. (2) and (3) respectively, as follows:

$$\mu = \frac{\ln X_2 - \ln X_1}{t_2 - t_1} \tag{2}$$

$$\upsilon = \frac{X_2 - X_1}{t_2 - t_1} \tag{3}$$

Where X_2 is the microalgae biomass dry weight at time t_2, and X_1 is the microalgae biomass dry weight at time t_1.

Microalgae CO_2 fixation rate (R_{CO2} mg $L^{-1}h^{-1}$) is calculated by the following Eq. (4).

$$R_{CO_2} = \frac{T_2 - T_1}{t_2 - t_1} \left(\frac{M_{CO_2}}{M_C} \right) \tag{4}$$

In which T_2 and T_1 are the total organic carbon concentration (TOC mg L^{-1}) at time t_1 and t_2, respectively. M_{CO2} represents the molecular weight of CO_2, and M_C represents the molecular weight of carbon. The total organic carbon concentration of microalgae was measured through a Total Organic Carbon/Total Nitrogen Analyzer (Multi N/C 2100 analyzer, Analytikjena, Germany).

Extracellular polymeric substances (EPS) consist of two parts, one loosely bound and the other tightly bound to the surface of the microalgae cells (Nguyen et al., 2020), from this EPS were extracted in two steps by the method from Barranguet et al. (2004). The total EPS of microalgae was collected by combining the supernatant after centrifugation of the two solutions. While the concentration of polysaccharides in EPS was obtained by the standard Eq. (5) through a fitting. Proteins were measured by the method (Rosero-Chasoy et al., 2022) and obtained by the standard Eq. (6).

$$PS = 0.0906 \times OD_{485} + 0.0676 \tag{5}$$

$$PN = 147.07 \times OD_{595} - 21.28 \tag{6}$$

In which PS (g L^{-1}) is the polysaccharide concentration and OD_{485} is the optical density of the polysaccharide sample, PN (mg L^{-1}) is the protein concentration and OD_{680} is the optical density of the protein sample.

2.2. Auto-agglomeration characterization

During the incubation process, the microalgae cells in suspension did not settle due to the mixing effect of the bubbling on the microalgae solution. The aliquots of the supernatant were taken at a depth of 5.0 cm from the liquid before and after stopping the bubbling for one hour. The auto-agglomeration ratio *AR*, %) of *C. sorokiniana* MB-1 was calculated below Eq. (7).

$$AR = \frac{C_i - C_t}{C_i} \times 100\ \% \quad (7)$$

Which C_i is the optical density of microalgae suspension before stopping aeration at 680 nm, and C_t is the optical density of microalgae suspension after stopping aeration for one hour at 680 nm.

The agglomerated microalgae particles in suspension were counted. An appropriate amount of microalgae suspension was aspirated and filtered on filter paper. After the water on the filter paper surface has evaporated completely, microalgae particle size is obtained by microscopy, then counted data through ImageJ.

2.3. Microalgae cells' surface characteristics

The determination of microalgae surface characteristics included the observation of microalgae surface morphology and the measurement of microalgae surface potential and fourier infrared spectra. The morphology of the microalgae surface was measured by microscopy (Olympus: IX81, Japan) and scanning electron microscopy (SEM, JEOL, JSM-7800F FEG, Japan). The SEM samples were performed according to Liu et al. (2020).

The surface of microalgae cells was analyzed by Flourier-transform infrared spectroscopy (FTIR, iS10 FT-IR spectrometer, Nicoli, America). Microalgae cells were placed on the sample holder to be measured for a wave number range of 400–4000 cm^{-1} after drying at 75 °C. The resolution of the spectrometer was 4 cm^{-1}, the signal-to-mania ratio was 50000:1, and 32 scans were taken.

2.4. Microalgae cells' surface zeta potential

The surface zeta potential was measured by a zeta potential analyzer (Nano ZS90, Mastersizer, UK). Different pH microalgae suspensions were prepared by taking fresh microalgae cultures and adding the appropriate amount of HCl and NaOH. The electrostatic repulsive double layer (G^{EL}) and Lewis acid-base (W^{AB}) on the surface of microalgae can be obtained by eDLVO theoretical formula (Chen et al., 2021). The contact angles of slides covered with microalgae were measured using the three liquids (Liu et al., 2016) in Table 1, and the contact angles of cells with the three above-mentioned solvents were applied to calculate their surface energy components (γ^{LW}, γ^{+}, and γ^{-}) according to Lifshitz-van der Waals/Lewis acid-base (LW-AB) approach (Chen et al., 2021). The microalgae cells used to measure contact angles were taken from culture suspensions, washed gently with deionized water to remove the surface medium, and placed in a natural environment (25 °C) to make thin slices of microalgae cells.

Table 1
The surface energy of three liquids and *C. sorokiniana* MB-1 cells. (mJ m^{-2}).

Liquid	γ_L	γ_L^{LW}	γ_L^{+}	γ_L^{-}
Water	72.8	21.8	25.5	25.5
Formamide	58	39	2.28	39.6
Diiodomethane	50.8	50.8	0	0
Solid	γ_S	γ_S^{LW}	γ_S^{+}	γ_S^{-}
C. sorokiniana MB-1		40.93	1.21	19.55

2.5. Microalgae metabolism measurement and analysis

Samples for non-targeted metabolomics were taken from fresh microalgal suspensions cultured up to day 5, and three parallel samples were taken from microalgae cultivated with 15% and 2% CO_2, respectively. The subsequent sample processing and measurement operations and data analysis were carried out according to the method of Yuan et al (2012).

3. Results and discussion

3.1. Microalgae periodical auto-agglomeration characteristics under different concentrations of carbon dioxide

The auto-agglomeration phenomenon of *C. sorokiniana* MB-1 was observed in different growth phases cultivated with 15% and 2% CO_2 (Fig. 1(a and b)), including the adaption phase (during the cultivation period of 0–1 day), the logarithmic phase (during the cultivation period of 2–5 day) and the stabilization phase (during the cultivation period of 6–7 day). Comparing the microalgae auto-agglomeration with different growth periods, it was found that there was the same auto-agglomeration ratio (20%) during the adaptation period under different concentrations of CO_2. However, there was a significant difference in microalgae auto-agglomeration during the stabilization phase under different concentrations of CO_2. Microalgae cells agglomerated and deposited at the bottom of the PBR steeply after the mixed gas bubble stopped, and the microalgae auto-agglomeration ratio even reached 100% under 15% CO_2. While microalgae cells cultivated with 2% CO_2 hardly agglomerated in this phase. Thus, it indicated that *C. sorokiniana* MB-1 cells were more likely to agglomerate and sediment in the stabilization phase under 15% CO_2. To further investigate more phenomenon of microalgae auto-agglomeration, the distribution characteristics of microalgae agglomerate particle size were necessary.

Microalgae agglomerated particle characteristics at different phases of cultivation were shown in Fig. (Fig. 1(c and d)). During the stabilization phase, the auto-agglomeration particles of microalgae cultivated with 15% CO_2 were larger and the proportion of large-size particles was higher, the microalgae within the field of view of the microscope are all essentially in the same floccule. In contrast, the auto-agglomeration particles of microalgae cultivated with 2% CO_2 were smaller and more loosely bound (Fig. 1(c)). In detail, the distribution of microalgae auto-agglomeration particles at each phase was shown in Fig. 1(d). Microalgae flocs agglomerated significantly at >50 μm^2 (Matsuda et al., 2016), during the adaptation phase, 92% and 95% of microalgae particles' size was >50 μm^2 when incubated at 15% CO_2 and 2% CO_2, respectively. During the stabilization period, the settling particles' size cultivated with 15% CO_2 was all above 50 μm^2, the settled microalgae cells were all agglomerated together at this phase, and it's advantageous for microalgae harvest (Yin et al., 2020). But, auto-agglomeration might result in a negative effect on microalgae cultivation (Cunha et al., 2020). Therefore, it's necessary to find out whether the microalgae growth and CO_2 fixation rate were reduced or not.

3.2. Microalgae growth different response to carbon dioxide

3.2.1. Microalgae growth and carbon sequestration characteristics

It's quite essential to keep microalgae growth positive when the cells were cultivated with a high concentration of CO_2 (Chen et al., 2023). Fig. 2 showed microalgae *C. sorokiniana* MB-1 carbon sequestration and growth characteristics during the whole cultivation phase. The results (Fig. 2(a and b)) showed that *C. sorokiniana* MB-1 maximum biomass was 3.27 g L^{-1} and the maximum carbon sequestration rate up to145 mg $L^{-1}h^{-1}$ under 15% CO_2, and compared to microalgae cultivated with 2% CO_2, these values increased 15.5% and 16% respectively. Analyzed in combination with Fig. 2(a and c), the biomass accumulation of microalgae was low (<1 g L^{-1}) in the adaptation phase, and a large number of

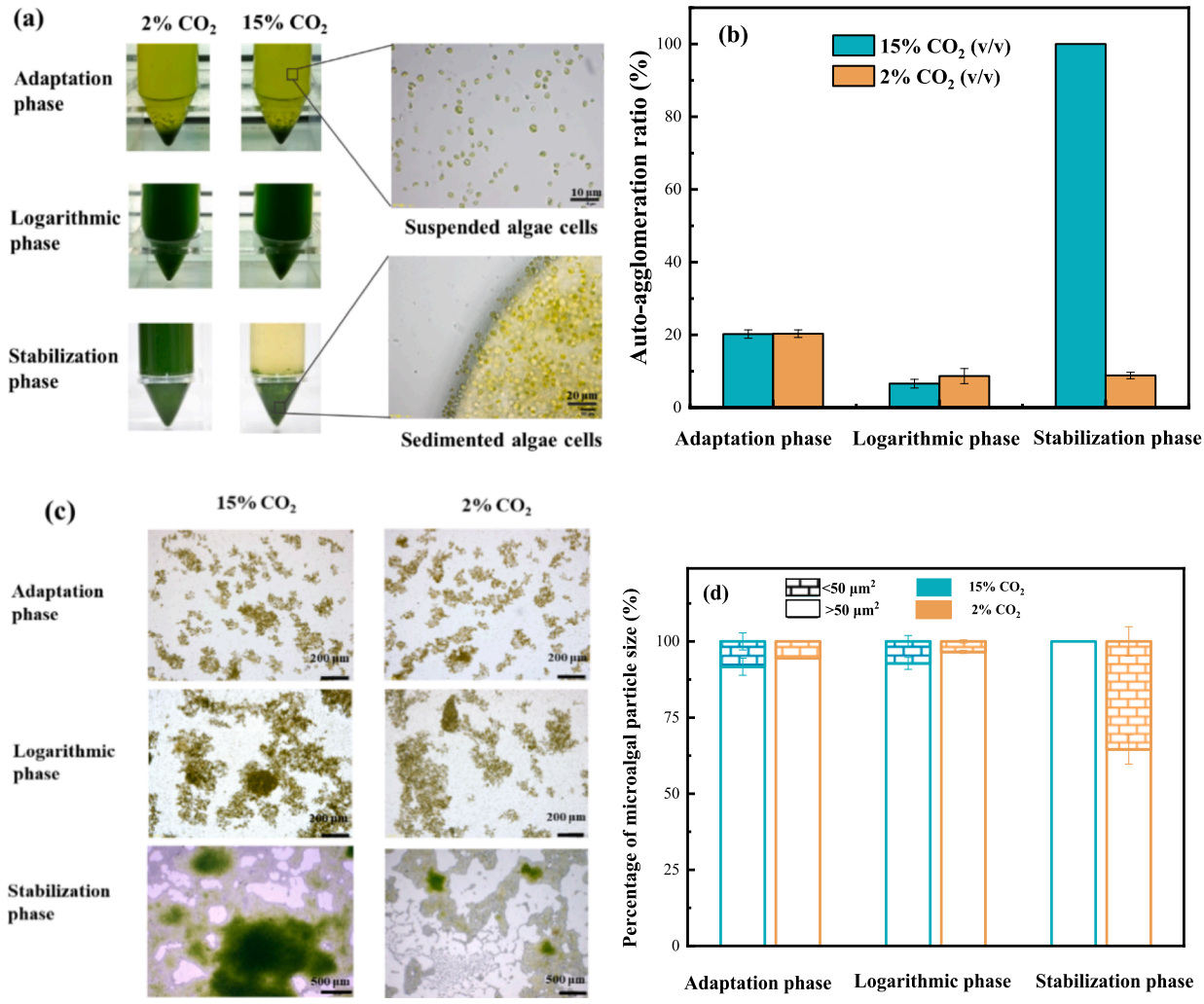

Fig. 1. Auto-agglomeration and particle characteristics of *C. sorokiniana* MB-1 during different cultivation phases (a) Microalgae cells' auto-agglomeration phenomenon, (b) Microalgae auto-agglomeration ratio; (c) Microalgae particles in auto-agglomeration; (d) Distribution of particles.

CO_2 (769 mg L^{-1}) was dissolved in the medium, the dissolved CO_2 in the medium decreased by 40 % under 15% CO_2. Under the same medium supplied, the maximum biomass of *Chlorella* cultivated with 15% CO_2 in the research of Qin et al. (2023) was 1.567 g L^{-1}. While the maximum biomass of *C. sorokiniana* MB-1 in this research was 3.27 g L^{-1}, this supported that *C. sorokiniana* MB-1 can be effectively grown and carbon sequestered under 15% CO_2.

The pH value affecting the surface electric potential of microalgae further allowed differences in electrostatic and acid-base hydrodynamic forces between cells (Wang et al., 2022). The trend of suspension pH was shown in Fig. 2(d), the pH of the microalgae suspension rapidly decreased from 7.33 to 6.03 due to the 15% CO_2, and then the solution pH rebounded due to the utilization of organic carbon by microalgae (Cao et al., 2019). To obtain the state of *C. sorokiniana* MB-1 at different pH, the following studies were carried out.

3.2.2. *Differences in energy barriers on microalgae cells' surface*

A certain concentration of microalgae solution was taken and the same concentration of microalgae suspension was prepared by HCl and NaOH solution to different pH (3–11). The auto-agglomeration ratio of *C. sorokiniana* MB-1 under these samples was shown in Fig. 3(a and b). It was inferred that the microalgae cells would agglomerate to varying degrees in either over-acidic (pH <4) or over-alkaline (pH >9) environments, especially in over-acidic environments where the microalgae would agglomerate rapidly, and it's same with other researches (Wei et al., 2020; Zhang et al., 2016). The microalgae cells' surface ζ-potential and auto-agglomeration ratio at different pH were shown in Fig. 3(c). When microalgae cells were in an over-acidic or over-alkaline environment, the microalgae cells' negative potential decreased from –23 mV to −15 mV, when the pH of microalgae suspension decreased from 7 to 3, and the microalgae auto-agglomeration ratio increased from 1% to 53 %, respectively. The results of calculating electrostatic action on microalgae cells' surface was shown in Fig. 3(d). The electrostatic action on *C. sorokiniana* MB-1 cells at pH 7 was 25.54% higher than at pH 3. The electrostatic force exhibited between microalgae cells was repulsive, the lower the electronegativity of the microalgae cells' surface, the weaker the repulsive force between microalgae cells, and the cells were more likely to agglomerating together, which eventually led to the microalgae cells' auto-agglomeration (Yuan et al., 2019).

Based on e-DLVO theory, the surface energy barriers between microalgae cells at different pH values were obtained under theoretical calculations, Fig. 3(e) showed the interaction energies between microalgae cells with a pH of 5. When the cell spacing was 3 nm, the microalgae energy barrier reaches a maximum of 797 kT, and the microalgae cells need to gain a large enough kinetic energy can cross this barrier to auto-agglomerate. According to Fig. 3(f), the energy barrier of *C. sorokiniana* MB-1 peaked at over 800 kT at pH 7–9 and decreased at all other pH values. It meant that microalgae cells auto-agglomerate and sediment more easily when the pH of the culture environment was beyond 7–9.

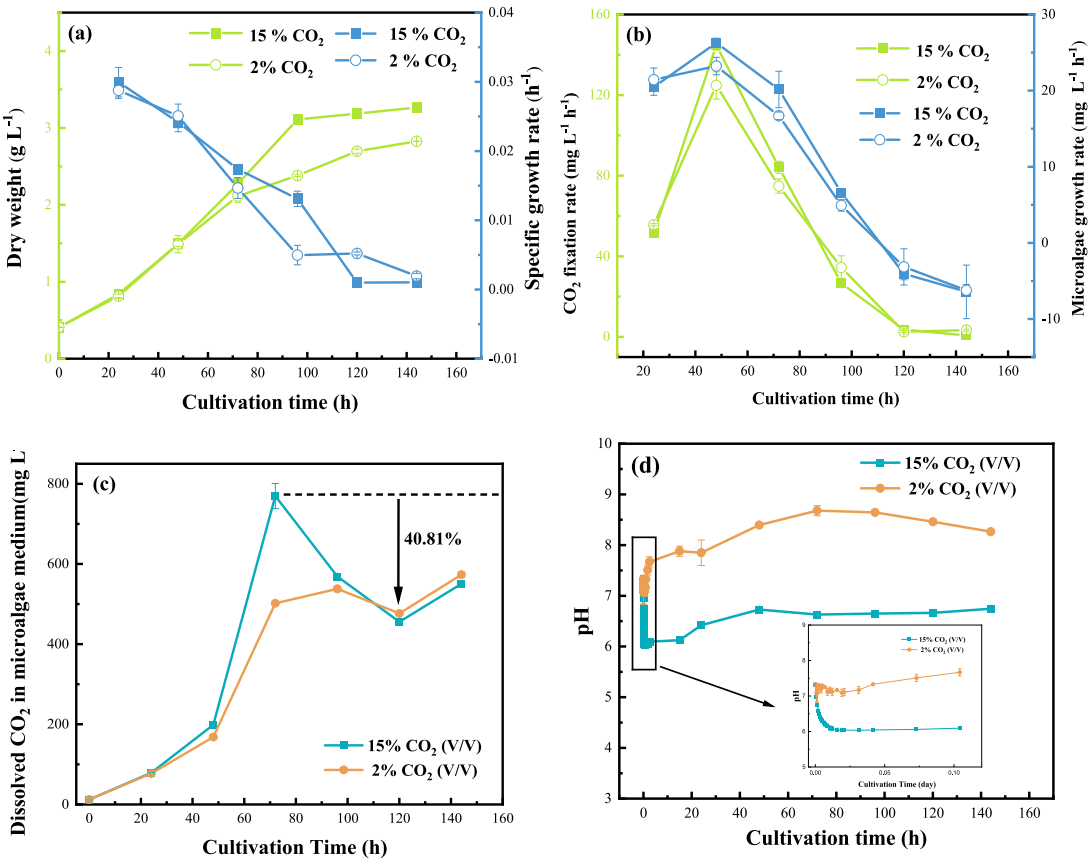

Fig. 2. Carbon sequestration and growth characteristics of *C. sorokiniana* MB-1. (a) Microalgae dry weight and specific growth rate; (b) Microalgae CO_2 fixation rate and growth rate; (c) Dissolved CO_2 in the medium; (d) pH trend of the medium.

Therefore, the culture solution pH during the adaptation phase will be lower than 7 under 15% CO_2, which reduced the energy barrier between microalgae cells and made the microalgae cells more prone to auto-agglomerate during the adaptation phase.

3.3. Contribution of microalgae extracellular polymeric substances to auto-agglomeration

EPS on the microalgae cells' surface can aggravate auto-agglomeration by causing cells to bond together (Wang et al., 2022). *C. sorokiniana* MB-1 cells' characteristics with an optical microscope and scanning electron microscope, there were both auto-agglomerated cells in the PBR's bottom and individual cells free in the suspension (see supplementary material). Auto-agglomerated microalgae cells were surrounded by EPS which held the microalgae cells together, resulting in a tighter and stronger agglomeration of microalgae cells. Further observation of the auto-agglomerated cells state by SEM showed that the surface of the microalgae cells was covered by EPS. The EPS acted as a flocculent to the adhesion of numerous algae cells together and continuously netted and swept more algae cells, which sank due to gravity and eventually formed larger auto-agglomerated microalgae clusters that were aggregated at the PBR's bottom (Cheah & Chan, 2021). While the suspended microalgae cells' surface did not have the presence of flocs, the cells did not sink under the combined effect of electrostatic repulsion, gravity, and other forces (Zhang et al., 2013). Accordingly, this part of the microalgae cells had a poor agglomeration capacity and was mostly free in the suspension.

The functional groups' absorbance on *C. sorokiniana* MB-1 cells' surface and their corresponding peaks were measured by FTIR spectroscopy at 500–4000 cm^{-1} (see supplementary material). The region of 3000–2850 cm^{-1} is C-H stretching vibration, 1465–1340 cm^{-1} is C-H bending vibration, CH_2 stretching vibration in the range of 3100–2800 cm^{-1} implies the presence of lipids (Paul Dumas, 2003). The region of 1600–1800 cm^{-1} is mainly the characteristic band of proteins, and the region from 1200 to 900 cm^{-1} indicates the vibrational bands of CH_3 and CH_2 on the polysaccharide moiety (Nathan Yee et al., 2003). The position and height of absorption peaks in the 1600–1800 cm^{-1} region were different between cells cultivated with 15% CO_2 and 2% CO_2, which demonstrated that the change of protein species and concentration on the microalgae cells' surface might cause by 15% CO_2. Compared the microalgae cells' IR functional group profiles with 2% CO_2 culture and EPS eluted, their peaks were the same, it revealed that the EPS of microalgae cultivated with 2% CO_2 was not tightly bound to the cells, while EPS of microalgae cells cultivated with 15% CO_2 did lead to agglomeration and sedimentation.

The Extracellular polysaccharides (ex-PS) concentration was basically at the same level under different CO_2 concentrations, while the extracellular proteins (ex-PN) content secreted by microalgae cells cultivated with 15% CO_2 was higher than 2%, which was increased by 20–30% (Fig. 4(a)). And the total organic carbon concentration of microalgae EPS cultivated with 15% CO_2 was up to 643 mg L^{-1}, also higher than 2% CO_2 (Fig. 4(b)). Among EPS components, proteins and polysaccharides made the main contribution to the agglomeration and adhesion of microalgae cells (Salim et al., 2014). Ex-PS promoted microalgae cells agglomerated, and ex-PN functioned in stabilizing the agglomerated microalgae cell particles, the higher proteins concentration was, the more stable auto-agglomerated cell clusters were (Chen et al., 2007; Seviour et al., 2009). In addition to the concentration, the ratio of EPS components also has a significant effect on microalgae auto-agglomeration. The ratio of extracellular polysaccharides to extracellular proteins (ex-PS/ex-PN) shown in Fig. 4(b), the ex-PS/ex-PN of *C. sorokiniana* MB-1 cultivated with 15% CO_2 was always lower than 2%

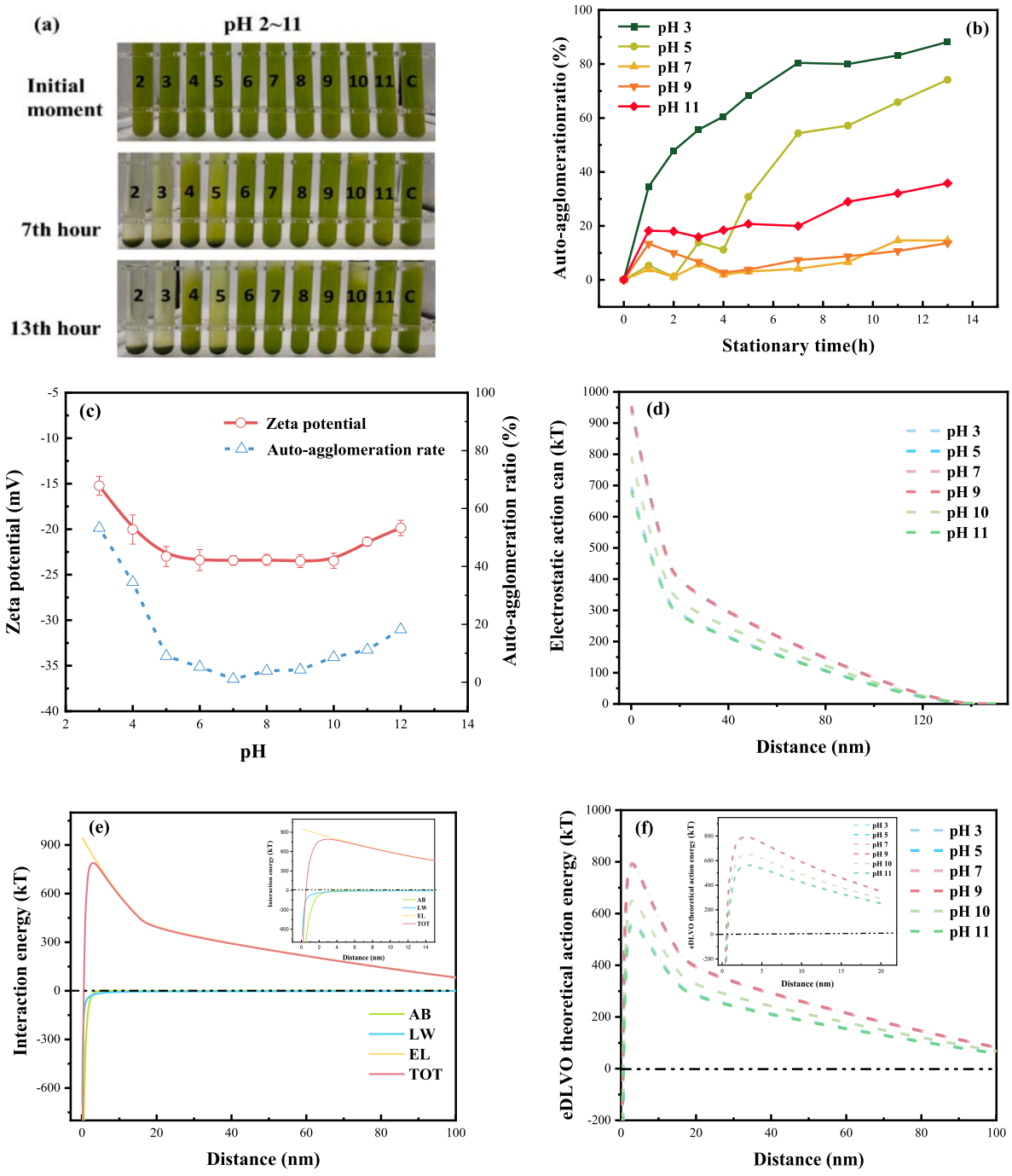

Fig. 3. Energy barriers of *C. sorokiniana* MB-1 microalgae cells surface at different pH. (a) Auto-agglomeration at different stationary times (b) Auto-agglomeration ratio at different stationary times; (c) Zeta potential and auto-agglomeration ratio at 2nd hour; (d) Electrostatic action can between microalgae cells; (e) The interaction energies between microalgae cells at pH of 5; (f) eDLVO theoretical action energy.

in the stabilization phase. The greater ex-PS/ex-PN, the smaller zeta potentials for the total EPS or its fractions, and the higher isoelectric point values for EPS fractions (Yuan & Wang, 2012). Thus, the microalgae auto-agglomeration capacity at the stabilization phase was sharply increased under 15% CO_2, and it's mainly attributed to the EPS concentration (mainly ex-PN) increased and ex-PS/ex-PN reduced, as illustrated in Fig. 4(c).

The morphology of EPS might be an essential cause of microalgae auto-agglomeration. As shown in Fig. 4(d), the morphology of microalgae EPS cultivated with 15% CO_2 was principally sheet-like, it coiled the cells together. The cells carried by such extracellular secretions were hard to escape from the agglomerated particles and the agglomerated particles would be more stable. In addition, the morphology of microalgae EPS cultivated with 2% CO_2 was clumpy, and cells were bridged together by EPS to form cellular agglomerates, which were relatively unstable and could be separated by a certain shearing force. The agglomeration effect of microalgae cells under different EPS forms was shown schematically in Fig. 4(e).

On the one hand, microalgae produced more extracellular proteins under 15% CO_2, which acted as an adhesive between microalgal cells. On the other hand, the form of microalgae cells' EPS was lamellae under 15% CO_2, which made microalgae cells agglomerate more firmly.

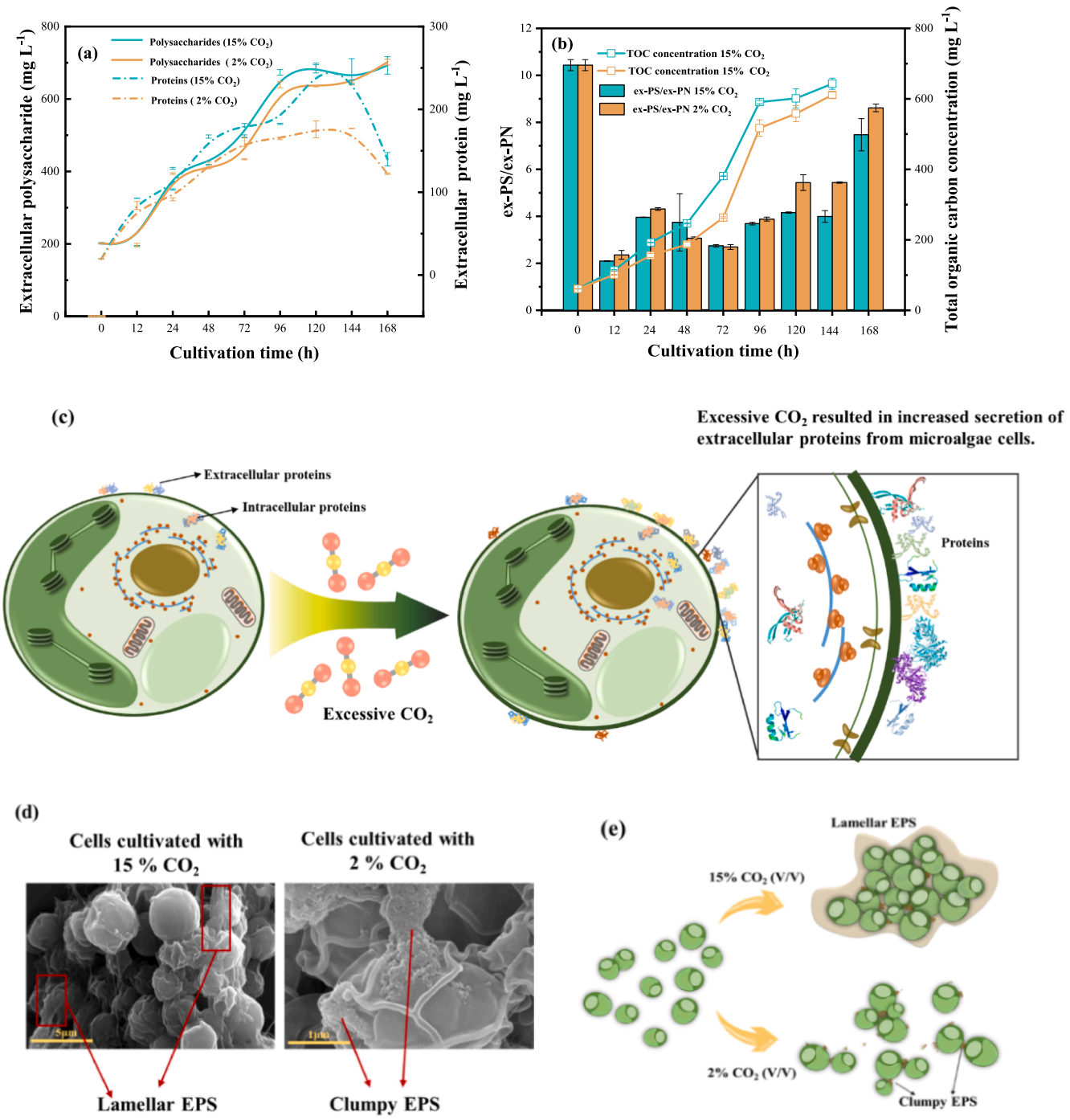

Fig. 4. Characteristics of EPS (a) Ex-PN and ex-PS concentrations; (b) Ex-PS/ex-PN; (c) More ex-PN secreted under 15% CO_2; (d) Cellular auto-agglomeration morphology; (e) Cellular auto-agglomeration schematic.

3.4. Characterization of microalgae extracellular polymeric substances synthesis

As sustainable biomass, the main available components of microalgae are proteins, polysaccharides, and lipids. The energy substance content in microalgae cells is crucial for the subsequent utilization of microalgae (Amjith & Bavanish, 2022; Das et al., 2021). To investigate whether changes in ex-PN and ex-PS affected intracellular polysaccharide (in-PN) and intracellular protein (in-PN) content, the microalgae cells' in-PN and in-PS were measured (Fig. 5(a)). Comparing the in-PN and in-PS of microalgae cultivated with different concentrations of CO_2, the in-PS content of microalgae cultivated with 15% CO_2 (maximum: 36 mg g^{-1}) was always slightly higher than that at 2% CO_2 (maximum: 35 mg g^{-1}), and the in-PN contents in these two situations were same (14 mg g^{-1}). Thus, the increase of ex-PN did not lead to the decrease of microalgae in-PN cultivated with 15% CO_2, while the microalgae in-PS increased due to the high carbon supplied. That was, the content of microalgae protein production (both in-PN and ex-PN) increased 20% under 15% CO_2.

The metabolism differences of microalgae cultivated with 15% and 2% CO_2 were compared, as shown in Fig. 5(b), the numbers of sign-up and sign-down metabolite levels accounted for 10.56% and 4.44%, respectively. The metabolism differences were primarily in the biosynthesis of amino acids, arginine biosynthesis, phenylalanine, tyrosine,

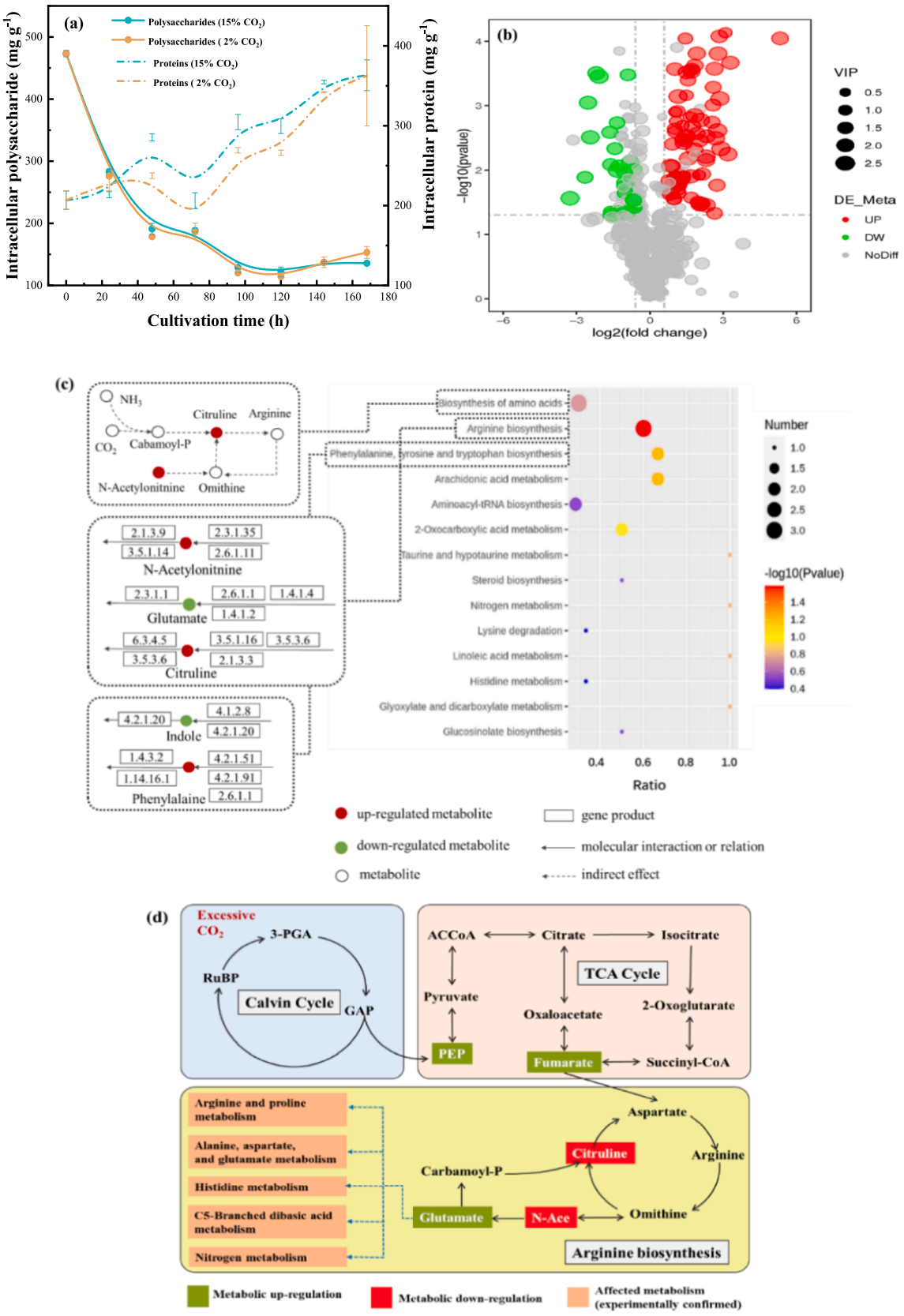

Fig. 5. Metabolism of *C. sorokiniana* MB-1 under 15% and 2% CO_2. (a) In-PN and in-PS concentrations; (b) Volcano plot of metabolites; (c) Differential metabolite enrichment bubble plots; (d) Differences of metabolism.

and tryptophan biosynthesis, arachidonic acid metabolism, aminoacyl-tRNA biosynthesis, 2-oxocaboxylic acid metabolism and so on (Fig. 5 (c)). Based on the above differences in microalgae metabolic cycles, a schematic representation of differences in the microalgae metabolism cultured at 15% and 2% CO_2 is presented in Fig. 5(d). Two important substances' metabolic levels in the triphosphate cycle were decreased, including PEP and fumarate. As precursors of the arginine biosynthesis, fumarate was probably caused by the increased metabolic levels of the downstream substances citrulline and N-Acetylomithine (N-Ace).

Arginine biosynthesis is mainly responsible for the fixation and conversion of nitrogen sources in microalgae metabolism, which is closely related to protein synthesis. An important nodal substance in arginine biosynthesis is glutamate (Yang et al., 2022). it was speculated that the decrease of glutamate was due to the increased metabolic level of its downstream substances, and the downstream metabolism associated with glutamate includes arginine and proline metabolism, alanine, aspartate, glutamate metabolism, histidine metabolism, C5-Branched dibasic acid metabolism, nitrogen metabolism and so on (Fig. 5(d)).

The increased metabolic levels of these metabolisms lead to microalgae proteins or peptides synthesis enhanced, as a result, there was a significant increase in the protein content and concentration of microalgae EPS cultivated with 15% CO_2.

4. Conclusion

This study investigated the mechanism and influence of microalgae cells' periodical auto-agglomeration that happened under a high concentration of CO_2 (15% CO_2). The auto-agglomeration during the adaption phase was caused by the decreased pH and the significant auto-agglomeration during the stabilization phase was caused by increased extracellular proteins and lamellar EPS. Microalgae maintained a high growth rate under 15% CO_2 and a remarkable agglomeration ratio during the stabilization phase, which is beneficial for the subsequent harvesting and utilization of biomass. These two features provide additional support for achieving efficient carbon sequestration by microalgae.

Declaration of Competing Interest

The authors declare that they have no known competing financial interests or personal relationships that could have appeared to influence the work reported in this paper

Data availability

Data will be made available on request.

Acknowledgments

This work was financially supported by research grants from the Innovative Research Group Project of the National Natural Science Foundation of China (No. 52021004), the State Key Program of National Natural Science of China (Grant No. 52236009), and the Fundamental Research Funds for the Central Universities (2022ZFJH004). We sincerely appreciate Prof. Jo-Shu Chang for providing the microalgae strain.

Appendix A. Supplementary data

Supplementary data to this article can be found online at https://doi.org/10.1016/j.biortech.2023.129120.

References

Amjith, L.R., Bavanish, B., 2022. A review on biomass and wind as renewable energy for sustainable environment. Chemosphere 293, 133579. https://doi.org/10.1016/j.chemosphere.2022.133579.

Awdhesh Kumar Mishra, R., Kodiveri Muthukaliannan, G., 2022. Role of microalgal metabolites in controlling quorum-sensing-regulated biofilm. Arch Microbiol 204 (3), 163. https://doi.org/10.1007/s00203-022-02776-2.

Barranguet, C., van Beusekom, S.A.M., Veuger, B., Neu, T.R., Manders, E.M.M., Sinke, J. J., Admiraal, W., 2004. Studying undisturbed autotrophic biofilms: still a technical challenge. Aquatic. Microbial. Ecology 34 (1), 1–9. https://doi.org/10.3354/ame034001.

Boussiba, S., Vonshak, A., 1991. Astaxanthin accumulation in the green-alga haematococcus-pluvialis. Plant Cell Physiol. 32 (7), 1077–1082. https://doi.org/10.1093/oxfordjournals.pcp.a078171.

Cao, X., Xi, Y., Liu, J., Chu, Y., Wu, P., Yang, M., Chi, Z., Xue, S., 2019. New insights into the CO_2-steady and pH-steady cultivations of two microalgae based on continuous online parameter monitoring. Algal Res. 38, 101370 https://doi.org/10.1016/j.algal.2018.11.021.

Chang, H., Fu, Q., Zhong, N., Yang, X., Quan, X., Li, S., Fu, J., Xiao, C., 2019. Microalgal lipids production and nutrients recovery from landfill leachate using membrane photobioreactor. Bioresour. Technol. 277, 18–26. https://doi.org/10.1016/j.biortech.2019.01.027.

Cheah, Y.T., Chan, D.J.C., 2021. Physiology of microalgal biofilm: a review on prediction of adhesion on substrates. Bioengineered 12 (1), 7577–7599. https://doi.org/10.1080/21655979.2021.1980671.

Cheah, W.Y., Show, P.L., Chang, J.-S., Ling, T.C., Juan, J.C., 2015. Biosequestration of atmospheric CO_2 and flue gas-containing CO_2 by microalgae. Bioresour. Technol. 184, 190–201. https://doi.org/10.1016/j.biortech.2014.11.026.

Chen, J.-H., Chen, C.-Y., Chang, J.-S., 2017. Lutein production with wild-type and mutant strains of *Chlorella sorokiniana* MB-1 under mixotrophic growth. Journal of the Taiwan Institute of Chemical Engineers 79, 66–73. https://doi.org/10.1016/j.jtice.2017.04.022.

Chen, X., Ding, B., Zhang, X., Yu, J., Song, M., Li, R., 2023. Regulatory mechanism of high-concentration CO(2) on polysaccharide accumulation in Tetradesmus obliquus cultured in sludge extract. Environ. Sci. Pollut. Res. Int. https://doi.org/10.1007/s11356-023-25554-z.

Chen, M.Y., Lee, D.J., Tay, J.H., 2007. Distribution of extracellular polymeric substances in aerobic granules. Appl. Microbiol. Biotechnol. 73 (6), 1463–1469. https://doi.org/10.1007/s00253-006-0617-x.

Chen, Z., Qiu, S., Yu, Z., Li, M., Ge, S., 2021. Enhanced Secretions of Algal Cell-Adhesion Molecules and Metal Ion-Binding Exoproteins Promote Self-Flocculation of *Chlorella sp.* Cultivated in Municipal Wastewater. Environ. Sci. Technol. 55 (17), 11916–11924. https://doi.org/10.1021/acs.est.1c01324.

Cunha, C., Silva, L., Paulo, J., Faria, M., Nogueira, N., Cordeiro, N., 2020. Microalgal-based biopolymer for nano- and microplastic removal: a possible biosolution for wastewater treatment. Environ. Pollut. 263 (Pt B), 114385 https://doi.org/10.1016/j.envpol.2020.114385.

Das, P.V.P.C., Mathimani, T., Pugazhendhi, A., 2021. Recent advances in thermochemical methods for the conversion of algal biomass to energy. Sci. Total Environ. 766, 144608 https://doi.org/10.1016/j.scitotenv.2020.144608.

Fu, J., Huang, Y., Xia, A., Zhu, X., Zhu, X., Chang, J.-S., Liao, Q., 2022. How the sulfur dioxide in the flue gas influence microalgal carbon dioxide fixation: From gas dissolution to cells growth. Renew. Energ. 198, 114–122. https://doi.org/10.1016/j.renene.2022.08.057.

IEA. 2023. Data and statistics, https://www.iea.org/data-and-statistics/data-tools/greenhouse-gas-emissions-from-energy-data-explorer. Last access date, 18 January 2023.

Jiutian, Z., Zhiyong, W., Jia-Ning, K., Xiangjing, S., Dong, X., 2022. Several key issues for CCUS development in China targeting carbon neutrality. Carbon Neutrality 1 (1), 1–20.

Koch, M., Bowes, G., Ross, C., Zhang, X.H., 2013. Climate change and ocean acidification effects on seagrasses and marine macroalgae. Global change biology 19 (1), 103–132. https://doi.org/10.1016/j.marpolbul.2022.113438.

Li, J., Li, B., Yang, J., 2021. Bio-Flocculation Property Analyses of Oleaginous Microalgae Auxenochlorella protothecoides UTEX 2341. Sustainability 13 (5). https://doi.org/10.3390/su13052885.

Liu, G., Jiang, R., You, J., Muir, D.C.G., Zeng, E.Y., 2020. Microplastic Impacts on Microalgae Growth: Effects of Size and Humic Acid. Environ. Sci. Technol. 54 (3), 1782–1789. https://doi.org/10.1021/acs.est.9b06187.

Liu, J., Tao, Y., Wu, J., Zhu, Y., Gao, B., Tang, Y., Li, A., Zhang, C., Zhang, Y., 2014. Effective flocculation of target microalgae with self-flocculating microalgae induced by pH decrease. Bioresour. Technol. 167, 367–375. https://doi.org/10.1016/j.biortech.2014.06.036.

Liu, J., Zhang, X., Tan, T., 2016. Mechanistically harvesting of *Chlorella vulgaris* and *Rhodotorula glutinis via* modified montmorillonoid. Bioresour. Technol. 218, 737–742. https://doi.org/10.1016/j.biortech.2016.07.016.

Ma, S., Zeng, W., Huang, Y., Zhu, X., Xia, A.o., Zhu, X., Liao, Q., 2022. Revealing the synergistic effects of cells, pigments, and light spectra on light transfer during microalgae growth: A comprehensive light attenuation model. Bioresour. Technol. 348, 126777.

Ma, S., Huang, Y., Zhang, B., Zhu, X., Xia, A., Zhu, X., Liao, Q., 2023. Comprehensive modeling and predicting light transmission in microalgal biofilm. J. Environ. Manage. 326, 116757.

Matsuda, S., Durney, A.R., He, L., Mukaibo, H., 2016. Sedimentation-induced detachment of magnetite nanoparticles from microalgal flocs. Bioresour. Technol. 200, 914–920. https://doi.org/10.1016/j.biortech.2015.11.006.

Moazami-Goudarzi, M., Colman, B., 2012. Changes in carbon uptake mechanisms in two green marine algae by reduced seawater pH. J. Exp. Mar. Biol. Ecol. 413, 94–99. https://doi.org/10.1016/j.jembe.2011.11.017.

Nathan Yee, L.G.B., Phoenix, V.R., Grant Ferris, F., 2003. Characterization of Metal-Cyanobacteria Sorption Reactions: A Combined Macroscopic and Infrared Spectroscopic Investigation. Environ. Sci. Technol. 38, 8. https://doi.org/10.1021/es0346680.

Nguyen, T.D.P., Vo, C.T., Nguyen-Sy, T., Tran, T.N.T., Le, T.V.A., Chiu, C.-Y., Sankaran, R., Show, P.L., 2020. Utilization of microalgae for self-regulation of extracellular polymeric substance production. Biochem. Eng. J. 159, 107616 https://doi.org/10.1016/j.bej.2020.107616.

Paul Dumas, L.M., 2003. The use of synchrotron infrared microspectroscopy in biological and biomedical investigations. Vib. Spectrosc. 32 (3–21) https://doi.org/10.1016/S0924-2031(03)00043-2.

Qin, Y., Wang, X.W., Lian, J., Zhao, Q.F., Jiang, H.B., 2023. Combination of non-sterilized wastewater purification and high-level CO(2) bio-capture with substantial biomass yield of an indigenous Chlorella strain. Sci. Total. Environ. 873, 162442 https://doi.org/10.1016/j.scitotenv.2023.162442.

Rosero-Chasoy, G., Rodriguez-Jasso, R.M., Aguilar, C.N., Buitron, G., Chairez, I., Ruiz, H. A., 2022. Growth kinetics and quantification of carbohydrate, protein, lipids, and chlorophyll of *Spirulina platensis* under aqueous conditions using different carbon and nitrogen sources. Bioresour. Technol. 346, 126456 https://doi.org/10.1016/j.biortech.2021.126456.

Salim, S., Kosterink, N.R., Tchetkoua Wacka, N.D., Vermue, M.H., Wijffels, R.H., 2014. Mechanism behind autoflocculation of unicellular green microalgae Ettlia texensis. J. Biotechnol. 174, 34–38. https://doi.org/10.1016/j.jbiotec.2014.01.026.

Seviour, T., Pijuan, M., Nicholson, T., Keller, J., Yuan, Z., 2009. Gel-forming exopolysaccharides explain basic differences between structures of aerobic sludge granules and floccular sludges. Water Res. 43 (18), 4469–4478. https://doi.org/10.1016/j.watres.2009.07.018.

Solovchenko, A., Gorelova, O., Selyakh, I., Pogosyan, S., Baulina, O., Semenova, L., Chivkunova, O., Voronova, E., Konyukhov, I., Scherbakov, P., 2015. A novel CO_2-tolerant symbiotic Desmodesmus (Chlorophyceae, Desmodesmaceae): Acclimation to and performance at a high carbon dioxide level. Algal Res. 11, 399–410. https://doi.org/10.1016/j.algal.2015.04.011.

Wang, Q., Shen, Q., Wang, J., Zhao, J., Zhang, Z., Lei, Z., Yuan, T., Shimizu, K., Liu, Y., Lee, D.-J., 2022. Insight into the rapid biogranulation for suspended single-cell microalgae harvesting in wastewater treatment systems: Focus on the role of extracellular polymeric substances. Chem. Eng. J. 430, 132631 https://doi.org/10.1016/j.cej.2021.132631.

Wei, C., Huang, Y., Liao, Q., Xia, A., Zhu, X., Zhu, X., 2020. Analysis of the energy barrier between Chlorella vulgaris cells and their interfacial interactions with cationic starch under different pH and ionic strength. Bioresour. Technol. 304, 123012 https://doi.org/10.1016/j.biortech.2020.123012.

Yang, R., Wei, D., Pohnert, G., 2022. Nitrogen utilization analysis reveals the synergetic effect of arginine and urea in promoting fucoxanthin biosynthesis in the mixotrophic marine diatom Phaeodactylum tricornutum. Frontiers in Marine Science 9. https://doi.org/10.3389/fmars.2022.947726.

Yang, F., Xiang, W., Fan, J., Wu, H., Li, T., Long, L., 2015. High pH-induced flocculation of marine Chlorella sp. for biofuel production. J. Appl. Phycol. 28 (2), 747–756. https://doi.org/10.1007/s10811-015-0576-7.

Yin, Z., Zhu, L., Li, S., Hu, T., Chu, R., Mo, F., Hu, D., Liu, C., Li, B., 2020. A comprehensive review on cultivation and harvesting of microalgae for biodiesel production: Environmental pollution control and future directions. Bioresour. Technol. 301, 122804 https://doi.org/10.1016/j.biortech.2020.122804.

Yuan, M., Breitkopf, S.B., Yang, X., Asara, J.M., 2012. A positive/negative ion-switching, targeted mass spectrometry-based metabolomics platform for bodily fluids, cells, and fresh and fixed tissue. Nat. Protoc. 7 (5), 872–881. https://doi.org/10.1038/nprot.2012.024.

Yuan, D.-Q., Wang, Y.-L., 2012. Study on the stratification components of extracellular polymeric substances (EPS) in activated sludge and their variation characteristics in physicochemical properties. Huanjing Kexue 33 (10), 3522–3528.

Yuan, H., Zhang, X., Jiang, Z., Chen, X., Zhang, X., 2019. Quantitative Criterion to Predict Cell Adhesion by Identifying Dominant Interaction between Microorganisms and Abiotic Surfaces. Langmuir 35 (9), 3524–3533. https://doi.org/10.1021/acs.langmuir.8b03465.

Zhang, X., Jiang, Z., Chen, L., Chou, A., Yan, H., Zuo, Y.Y., Zhang, X., 2013. Influence of cell properties on rheological characterization of microalgae suspensions. Bioresour. Technol. 139, 209–213. https://doi.org/10.1016/j.biortech.2013.03.195.

Zhang, X., Zhao, X., Wan, C., Chen, B., Bai, F., 2016. Efficient biosorption of cadmium by the self-flocculating microalga Scenedesmus obliquus AS-6-1. Algal Res. 16, 427–433. https://doi.org/10.1016/j.algal.2016.04.002.